ISIJ International, Vol. 53 (2013), No. 7, pp. 1286–1288

Note

Inheritance of Dislocations and Crystallographic Texture during Martensitic Reversion into Austenite

Nobuo NAKADA,[1,2]* Reiji FUKAGAWA,[3]
Toshihiro TSUCHIYAMA,[1,2] Setsuo TAKAKI,[1,2]
Dirk PONGE[4] and Dierk RAABE[4]

1) Department of Materials Science and Engineering, Graduate School of Engineering, Kyushu University, 744 Moto-oka, Nishi-ku, Fukuoka, 819-0395 Japan. 2) International Institute for Carbon Neutral Energy Research (WPI-I2CNER), Kyushu University, 744 Moto-oka, Nishi-ku, Fukuoka, 819-0395 Japan.
3) Graduate Student of Engineering, Kyushu University, 744 Moto-oka, Nishi-ku, Fukuoka, 819-0395 Japan.
4) Max-Planck-Institute für Eisenforschung, Max-Planck-Str. 1, 40237 Düsseldorf, Germany.

(*Received on January 17, 2013; accepted on April 1, 2013*)

KEY WORDS: austenite; martensitic reversion; reversible martensitic transformations; crystallographic memory effect.

1. Introduction

When a maraging steel is austenitized, reversion from martensite back to austenite was reported to occur via a diffusionless shear mechanism (martensitic reversion).[1–4] A high Ni content decreases the T_0 temperature in such steels (T_0: temperature where the Gibbs free energies of martensite and austenite are equal), hence, suppressing diffusional transformation. It was further reported that the austenite formed by martensitic reversion (martensitically reversed austenite) is statically recrystallized by prolonged austenitization. This effect results in a considerable loss of strength and toughness after quenching, although the prior austenite grain size is markedly refined by the recrystallization.[2,4] In order to explain this phenomenon, it was suggested that martensitically reversed austenite contains a high dislocation density that may provide the driving force for primary recrystallization. It was suggested that the high dislocation density that is typical of maraging steel may contribute to the good mechanical property of this material class due to an ausforming-like effect as long as the recrystallization of the martensitically reversed austenite does not occur.[2–4] Besides these specific effects, the entire microstructural evolution and the toughening mechanisms occurring during martensitic reversion in such alloys remain unclear. Since austenite is an unstable phase in maraging steel at ambient temperature, its microstructure cannot be probed directly and austenite produced by martensitic reversion is usually difficult to access.

Previous authors succeeded to obtain the martensitically reversed austenite at ambient temperature through deformation-induced martensitic transformation in a meta-stable austenitic stainless steel.[5,6] It was found that the martensitically reversed austenite had a high dislocation density within the fine lath structure. However, it remained unclear whether the high dislocation density is inherent to the martensitic reversion mechanism itself or whether it is a microstructure that is inherited from prior cold-deformation of austenite that was used to induce martensitic transformation. In this study we aim at directly mapping martensitically reversed austenite without any deformation-induced martensitic transformation. For this purpose we use a novel approach of austenite stabilization using carbon. More specific, we introduce a new type of heat treatment to control austenite stability by precipitation and dissolution of carbide. This method allows us to directly access and map the inherent characteristics of martensitically reversed austenite in a 18%Ni–C steel (%=wt.%).

2. Heat Treatment, Alloy Designing and Experimental Procedure

Martensite transformations can be stimulated either by plastic deformation and/or by reducing the austenite stability. In our approach we aim at producing meta-stable austenite by formation of a second phase. Since carbon is a very effective austenite stabilizing element, it is plausible that carbide precipitation should destabilize austenite and hence induce a martensitic transformation upon cooling to ambient temperature. Therefore, we developed a heat treatment consisting of a three step solid-solution heat treatment sequence (STs) with the aim to modify the austenite stability of the matrix through the precipitation and dissolution of carbide, as drawn in **Fig. 1**(a). The key point in this heat treatment is the second ST that is employed to reduce the solute carbon content in the austenite matrix by a partial solution treatment in the austenite plus carbide two phase region. In order to stimulate a martensitic transformation in the entire specimen during heat treatment, the following conditions are required: (1) The austenite matrix has to be sufficiently stable at ambient temperature (R.T.) when the carbon is entirely in solid solution (Ms < R.T. at 1st ST, Ms: temperature where martensitic transformation starts); (2) Precipitation of carbide in the austenite plus carbide two phase region increases the T_0 temperature. As a result, the martensitic transformation fully occurs during the subsequent cooling (Mf > R.T. at 2nd ST, Mf: temperature where martensitic transformation finishes). The material selected for this study is a hypereutectoid steel with a large carbon solubility gap depending on the austenitizing temperature. A further condition is to stabilize the martensitically reversed austenite also down to ambient temperature. (3) The precipitated carbide (see step (2)) immediately dissolves into the austenite matrix again after martensitic reversion in order to restore the Ms and Mf temperatures to their initial values (Ms < R.T. at 3rd ST). For all processing steps it must be consider that

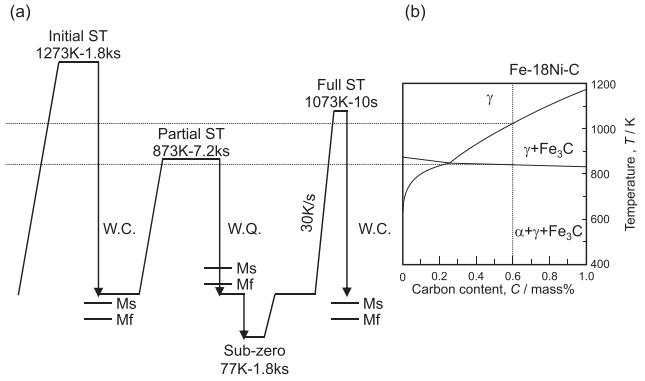

Fig. 1. (a) Heat treatment root to control austenite stability by precipitation and dissolution of carbide and (b) phase diagram of Fe-18%Ni–C alloy.

* Corresponding author: E-mail: nakada@zaiko.kyushu-u.ac.jp
DOI: http://dx.doi.org/10.2355/isijinternational.53.1286

additional microstructural changes, such as recovery and recrystallization, may take place within the austenite at elevated temperature.[2–4] Thus, cementite is used in the form of precipitated carbide to satisfy the third condition, because cementite dissolves more easily in the matrix rather than alloyed carbides. Following these considerations, a 18%Ni–C (%=wt.%) steel was selected as alloy appropriate for the heat treatment technique outline above. Figure 1(b) represents the equilibrium phase diagram of a 18%Ni–C steel calculated by *Thermo-calc*. (SSOL6 database). The equilibrium diagram reveals that the carbon solubility in austenite varies over a wide range depending on temperature and that it reaches a minimum of approximately 0.25 wt.% at around the eutectoid temperature[†1,†2]. Shibata *et al*. investigated the effects of the *Ms* temperature and of the carbon content on the morphology of martensite in the Fe–Ni–C system.[7] They observed that 0.25 wt.%C does not decrease the *Mf* temperature to ambient temperature, while a content of 0.6%C is high enough to stabilize austenite in 18Ni–C steel. Consequently, a 18%Ni-0.6%C steel (18.4%Ni-0.57%C-0.16%Mn; %=wt.%) was prepared and subjected to the heat treatment as detailed in (a). Firstly, the material was solution treated at 1 273 K in the austenite single phase region as initial state (Initial ST). Subsequently, the material was held at 873 K in the austenite plus cementite two phase region for 7.2 ks (ks: 10^3 seconds) to fully precipitate cementite, followed by water-quenching and low temperature quenching at 77 K to induce martensitic transformation (Partial ST). Finally, the so obtained material was re-heated at a heating rate of 30 K/s and held at 1 073 K in the austenite single phase region for 10 s, followed by water-cooling (Full ST). In this study, specimens after each of these steps (ST) are in the following referred to as Initial, Partial and Full ST materials, respectively. The phase fraction in each material was evaluated by X-ray diffraction and magnetization saturation methods. The microstructure was observed with optical and transmission electron microscopes (TEM). The crystallographic orientation of each phase was mapped by means of the electron back scattering diffraction (EBSD) method using a field emission scanning electron microscope JSM-6701F developed by JEOL Ltd..

3. Results and Discussion

Figure 2 shows optical micrographs and orientation imaging maps obtained by high resolution EBSD taken at a step size of 200 nm. The micrographs show the structure of the material in the Initial state (a, b), Partial state (c, d) and Full ST state (e, f). The orientation imaging maps display the only major phase, fcc or bcc, respectively. In the orientation imaging maps, high-angle grain boundaries are indicated as black lines. As examples of special interfaces (prior) austenite grain boundary and annealing twin boundary are indicated by arrows A and B, respectively. The Initial ST material (a) has a typical austenite single phase structure with annealing twin. Its austenite grain size amounts to several hundred micrometers. Additionally, EBSD map (b) reveals that the fcc crystal orientation is completely homogeneous, *i.e*. identical inside each of the grains. These results mean that the carbon was fully in solid solution in the austenite matrix, leading to sufficient stabilization of the austenite at room temperature. In the Partial state, the material seems to have been fully transformed into finely structured martensite (c). The volume fraction of retained austenite in this state was determined to be negligible by magnetization saturation method. The orientation map for the material in Partial ST state (d) indicates that the microstructure is lath martensite characterized by a complex arrangement of martensite packets and blocks, such as typically observed in high Ni martensite.[8,9] This means that the prior austenite grains were finely divided by high-angle packet and block boundaries after transformation. It is well known that the hardness of martensitic steel depends mainly on the carbon content. According to previous results,[10] approximately 0.25 wt.%C is estimated to be in solid solution in the Partial ST material according to its high hardness in this state (5.4 GPa). It is important to note that the Full ST material (e) was also identified as fully austenitic single phase structure. However, its microstructure appears to be profoundly different from the austenite substructure observed in the Initial ST material (a): In the Full ST material, the austenite exhibits a fine microstructure and its hardness exceeds that of the Initial ST material by more than 1.0 GPa. The orientation map (f) reveals that the Full ST material has a coarse austenite structure with annealing twins similarly to the Initial ST material (b), although some fine austenite grains surrounded by high-angle boundary are dispersed within the coarse microstructure as will be discussed below. It should be noted that the fcc crystal orientation seems to be not identical but slightly distributed in the coarse austenite structure, which may correspond to the fine microstructure observed by optical microscopy (e). For investigating the orientation distribution in the coarse austenite structure, TEM image of the Full ST material is shown in **Fig. 3**(a). For comparison with the Full ST material, the lath martensite structure of the Partial ST material is also shown in figure (b). The Full ST material (a) has a lath structure with 200 nm lath dimension

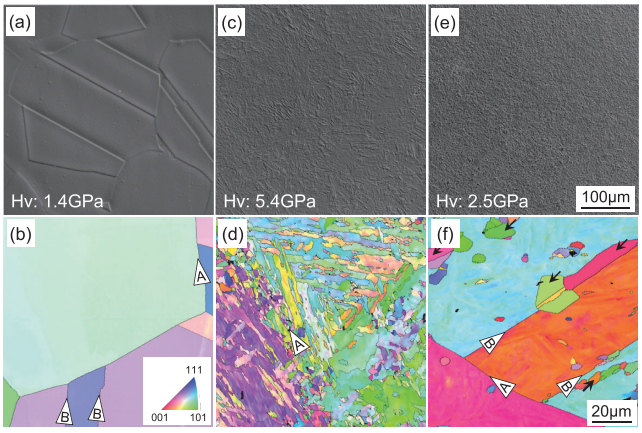

Fig. 2. Optical micrographs and orientation imaging maps of (a, b) Initial, (c, d) Partial and (e, f) Full S.T. materials.

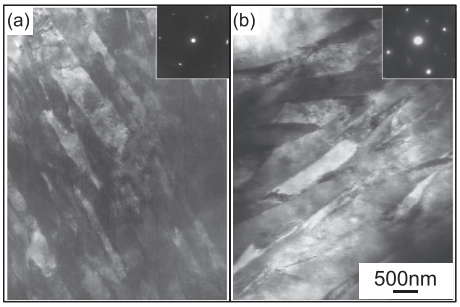

Fig. 3. TEM images showing lath structure in (a) Full ST and (b) Partial ST materials.

[†1]: The thermodynamic calculations suggest that actually graphite is actually the more stable phase compared to cementite, but we experimentally confirmed that cementite precipitates preferentially in this material.

[†2]: Since the diffusivity of Ni in austenite is quite low around 873 K, we assumed that para-cementite precipitates in austenite.

in width and contains a high dislocation density. In addition, the selected area electron diffraction pattern obtained from this area reveals a single diffraction pattern with a slight streaking. This indicates that all austenite laths have almost the same crystallographic orientation and the lath boundaries are characterized by low-angle misorientations of only a few degrees. Thus, such a small angle lath morphology explains the mesoscale crystallographic orientation distribution observed at a larger scale by EBSD in Fig. 2(f). Indeed, the average deviation of misorientation angle in lath austenite was evaluated at 0.54 degrees in the EBSD map. These microstructural features are similar to the features observed for the present lath martensite represented in (b).[11] We, hence, refer to the austenite structure as "lath austenite". The comparison between TEM images (a: Full ST material) and (b: Partial ST material) strongly suggests that the microstructure of the newly formed lath austenite was most likely inherited, *i.e.* carried over from the lath martensite. From these result, it can be concluded that the lath austenite in the Full ST material is a martensitically reversed austenite that formed from the preceding lath martensite.

However, it should be noted that the high-angle packet and block boundaries that originally existed in the lath martensite have disappeared in the lath austenite (see Figs. 2(d), 2(f), respectively). The reason is as follows: It is understood that several martensite variants with different orientation must form during the martensitic transformation in order to comply with the boundary conditions imposed by the neighboring microstructure. The total strain created by a set of martensite variants, each with its individual anisotropic martensitic transformation strain, is mutually compensated and hence matches the local boundary conditions more readily than the transformation of only one variant. Therefore in lath martensite, a prior austenite grain is subdivided by high-angle grain boundaries because each packet and block consists of different variants (*e.g.* out of the 24 K-S variants; K-S: Kurdjumov-Sachs). If all variants had the same orientation, not only lath boundaries but also packet and block boundaries would form low-angle grain boundaries. Therefore, the disappearance of high-angle packet and block boundaries in the lath austenite obtained after martensitic reversion clearly demonstrates that all martensite variants that were originally formed by a fcc→bcc martensitic transformation reverse into the new austenite during the bcc→fcc martensitic reversion with the same resulting orientation that the prior austenite grain had. This means that a crystallographic memory effect appears even in such an athermoelastic martensitic transformation of a ferrous material as in the present study (fcc→bcc→fcc reversible transformations in crystallography). It should be noted that some finely dispersed austenite grains appear in the Full ST material that do not obey this orientation re-transformation (see Fig. 2(f), as indicated by black arrows). These zones may have been formed around the originally dispersed cementite particles via a diffusional mechanism. The reason for this heterogeneity is that the cementite particles dissolved upon the heating imposed during the Full ST stage, which promoted diffusional reversion. We observed that such diffusional austenite formation can be suppressed with increasing heating rate, which is consistent with this explanation.

The microstructural evolution during the fcc→bcc→fcc reversible martensitic transformations is schematically illustrated in **Fig. 4**. Although the orientation of martensitically reversed austenite turns back to that of an original austenite portion including its original crystallographic orientation that it had before the transformations, a fine lath structure and a high dislocation density remain in the newly formed austenite. Both microstructural features that seem to be specific characteristics of lath austenite are inherited during the martensitic reversion. This is enabled by the athermal character of the lattice invariant deformation upon martensitic reversion.

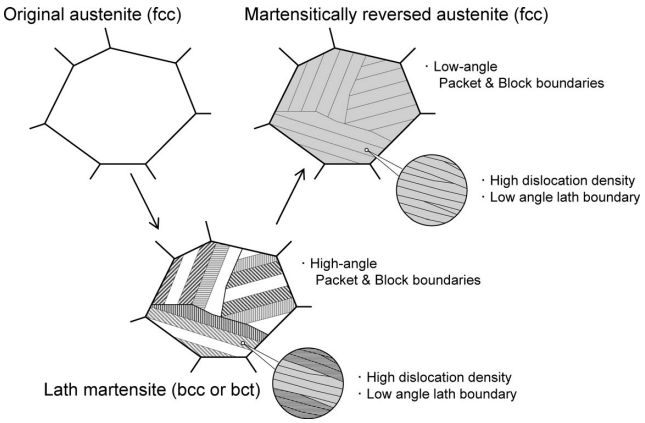

Fig. 4. Schematic illustration of microstructural evaluation during fcc→bcc→fcc reversible martensitic transformations.

4. Conclusions

A novel type of heat treatment to control austenite stability by precipitation and dissolution of carbide was applied to a 18%Ni-0.6%C steel (%=wt.%). The new method enabled us to study the inherent characteristics of austenite formed by martensitic reversion. The results obtained are summarized as follows:

(1) We observed a full fcc→bcc→fcc reversible martensitic transformations cycle. As a result of the specific heat treatment, the austenite that was formed by martensitic reversion remains stable at ambient temperature.

(2) The austenite formed by martensitic reversion has a fine lath structure with high dislocation density similar to lath martensite and it has the same crystallographic orientation as the original austenite grain from which the fcc→bcc→fcc transformation sequence started. This observation indicates that martensitic reversion follows an athermal, *i.e.* displacive mechanism.

Acknowledgement

This study was supported by Grant-in-Aid for Young Scientist (A) No. 22686065 (2010-2011) and Scientific Research (C) No. 24560852 (2012-2015) from Japan Society for the Promotion of Science and the International Institute for Carbon Neutral Energy Research (WPI-I2CNER), sponsored by the Japanese Ministry of Education, Culture, Sports, Science and Technology.

REFERENCES

1) Y. E. A. Fakina, L. V. Smirnov and V. D. Sadovskiy: *Phys. Met. Metallogr.*, **31** (1971), 199.
2) K. Hosomi, Y. Ashida, R. Atagi and H. Hato: *Trans. JIM*, *Suppl.*, **17** (1976), 87.
3) T. Maki, H. Morimoto and I. Tamura: *Tetsu-to-Hagané*, **65** (1979), 1598.
4) T. Tasuno, A. Koganei, K. Kuribayashi, T. Hasegawa and R. Horiuchi: *ISIJ Int.*, **36** (1996), 595.
5) K. Tomimura, S. Ueda, S. Takaki and Y. Tokunaga: *Tetsu-to-Hagané*, **77** (1991), 1519.
6) N. Nakada, D. Fukae, T. Kitaura, T. Tsuchiyama and S. Takaki: *Netsushori*, **47** (2007), 371.
7) A. Shibata: Doctor Thesis, Kyoto University, (2007).
8) T. Maki and I. Tamura: *Tetsu-to-Hagané*, **67** (1981), 852.
9) D. Raabe, D. Ponge, O. Dmitrieva and B. Sander: *Scr. Mater.*, **60** (2009), 1141.
10) G. Krauss: Hardenability Concepts with Application to Steel, ed. by D. V. Doane and J. S. Kirkaldy, AIME, New York, (1978), 229.
11) S. Morito, X. Huang, T. Furuhara, T. Maki and N. Hansen: *Acta Mater.*, **54** (2006), 5323.